Synthesis and Properties of the Sodium Lithium Silicate Silinaite

Klaus Beneke, Peter Thiesen, and Gerhard Lagaly*

Institute of Inorganic Chemistry, Kiel University, Olshausenstrasse 40, D-24098 Kiel, Germany

Received June 8, 1994[⊗]

A new sodium lithium silicate (as mineral silinaite) is synthesized from dispersions of silica in aqueous solutions of NaOH and LiOH at 90−150 °C. Synthetic samples of silinaite are characterized by X-ray powder diagrams, IR and MAS-NMR spectra, thermal dehydration, and gas adsorption measurements. Thermal dehydration produces an anhydrous lithium sodium silicate which melts at about 650 °C. The lithium and sodium ions can be exchanged by protons and alkylammonium ions. Exchange of the alkali metal ions by protons transforms silinaite into the H^+ form, into α-$H_2Si_2O_5$, or into a mixture of both acids. Formation of the acids largely increases the specific surface area. The H^+ form of silinaite contains considerable amounts of micropores. Water is continuously desorbed between room temperature and 1000 °C. The influence of kinetic factors (trapping of water molecules between the collapsing layers of the acid) is stronger than in silinaite. The acid only intercalates a few types of guest molecules, e.g. alkyl- and arylamines and basic heterocyclic compounds. The intracrystalline reactivity is as low as for other monophyllosilicic acids such as α- and β-$H_2Si_2O_5$ and the H^+ forms of kanemite and makatite.

Introduction

In spite of a great diversity of synthetic alkali silicates natural products were unknown until 1967 when Eugster[1] detected two hydrous sodium silicates which afterwards were named magadiite and kenyaite (Table 1). Later, makatite[2] and kanemite[3] were described. One anhydrous sodium silicate mineral is natrosilite.[4] Revdite and grumantite were described by Khomyakov et al.[5,6] The group of natural alkali silicates is now extended by silinaite which was identified and separated from many other minerals present in xenoliths at Mont Saint-Hilaire, Quebec, Canada.[7,8] Makatite and revdite were also found in these xenoliths.

A particular merit of the Canadian scientists is the determination of the crystal structure of silinaite[9] because only the structure of the makatite and revdite is known. (Revdite is a water soluble sodium silicate with a new, unique framework of $[SiO_4]$ tetrahedra.[10])

Silinaite is a monophyllosilicate consisting of layers of $[SiO_4]$ tetrahedra parallel to (001). The tetrahedral layer is a zweier single layer (classification of Liebau[11]) as in $Li_2Si_2O_5$ and the modifications of $Na_2Si_2O_5$. The lithium ions are held in tetrahedral coordination by the four oxygen ions of four $[SiO_4]$ tetrahedra and pull the layers together. The octahedra around the sodium ions consist of four water molecules and two oxygen ions which also belong to $[SiO_4]$ and $[LiO_4]$ tetrahedra. The $[NaO_6]$ octahedra bulge the layers somewhat apart so that the layers are slightly undulated. Makatite contains layers composed of vierer single chains which are highly convoluted.[12]

Table 1. Alkali Silicate Minerals

mineral	idealized composition
natrosilite	$Na_2Si_2O_5$
kanemite	$NaHSi_2O_5{\cdot}2H_2O$
revdite	$Na_2Si_2O_5{\cdot}5H_2O$
grumantite	$NaHSi_2O_5{\cdot}0.9H_2O$
silinaite	$NaLiSi_2O_5{\cdot}2H_2O$
makatite	$Na_2Si_4O_8(OH)_2{\cdot}4H_2O$
magadiite	$Na_2H_2Si_{14}O_{30}{\cdot}xH_2O$
kenyaite	$Na_2H_2Si_{20}O_{42}{\cdot}xH_2O$

Makatite, magadiite, and kenyaite are synthesized from dispersions of silica in aqueous solutions of NaOH or KOH between 70 and 150 °C.[13−19] Kanemite can be prepared by different routes.[20] A further method is to react a water glass solution with ethylene diamine or triethanol amine at 60 °C for 2−3 months. One of the potassium analogues of kanemite, $KHSi_2O_5$-II, forms from a mixture of potassium water glass solution and triethanol amine or ethanol. The lithium analogue of kenyaite, $Li_2H_2Si_{20}O_{42}{\cdot}xH_2O$, is obtained from mixtures of 1 mol of SiO_2, 1 mol of LiOH, and 40 mol of water at 100 °C.[21]

The characteristic property of the layered alkali silicates is the intracrystalline reactivity. Typical reactions are displacement

[⊗] Abstract published in *Advance ACS Abstracts,* January 15, 1995.

(1) Eugster, H. P. *Science* **1967**, *157*, 1177−1180.
(2) Sheppard, R. A.; Gude, A. J.; Hay, R. L. *Am. Mineral.* **1970**, *55*, 358−366.
(3) Johan, Z.; Maglione, G. F. *Bull. Soc. Fr. Mineral. Cristallogr.* **1972**, *95*, 371−382.
(4) Timoshenkov, I.; Menshikov, Y. P.; Gannibal, L. F.; Bussen, I. V. *Zap. Vses. Mineral. Ova.* **1975**, *104*, 317−324. See also: Fleischer, M. New Mineral Names: Natrosilite. *Am. Mineral.* **1976**, *61*, 339−340.
(5) Khomyakov, A. P.; Cherepivskaya, G. E.; Kurova, T. A.; Vlasyuk, V. P. *Zap. Vses. Mineral. Ova.* **1980**, *109*, 566−579. See also: Fleischer, M. New Mineral Names. *Am. Mineral.* **1982**, *67*, 1076.
(6) Khomyakov, A. P.; Korobitsyn, M. F.; Kurova, T. A.; Cherepivskaya, G. E. *Zap. Vses. Mineral. Ova.* **1987**, *116*, 244−248. See also: Puziewicz, J. New Mineral Names. *Am. Mineral.* **1988**, *73*, 440.
(7) Chao, G. Y.; Conlon, R. P.; Velthuizen, J. V. *Mineral. Rec.* **1990**, *21*, 363−368.
(8) Chao, G. Y.; Grice, J. D.; Gault, R. A. *Can. Mineral.* **1991**, *29*, 359−362.
(9) Grice, J. D. *Can. Mineral.* **1991**, *29*, 363−367.
(10) Rastsvetaeva, R. K.; Mikheeva, M. G.; Yamnova, N. A.; Pushcharovskii, D. Y.; Khomyakov, A. P. *Sov. Phys.—Crystallogr.* (*Engl. Transl.*) **1992**, *37*, 632−636; *Kristallografiya* **1992**, *37*, 1177−1184.
(11) Liebau, F. *Structural Chemistry of Silicates (Structure, Bonding, Classification)*; Springer Verlag: Heidelberg, Germany, 1985.
(12) Annehed, F.; Falth, L.; Lincoln, F. J. *Z. Kristallogr.* **1982**, *159*, 203−210.
(13) Lagaly, G.; Beneke, K.; Weiss, A. *Am. Mineral.* **1975**, *60*, 642−649.
(14) Beneke, K.; Lagaly, G. *Am. Mineral.* **1983**, *68*, 818−826.
(15) Beneke, K.; Lagaly, G. *Am. Mineral.* **1989**, *74*, 224−229.
(16) Schwieger, W.; Heyer, W.; Wolf, F.; Bergk, K.-H. *Z. Anorg. Allg. Chem.* **1987**, *548*, 204−216.
(17) Schwieger, W.; Heyer, W.; Bergk, K.-H. *Z. Anorg. Allg. Chem.* **1988**, *559*, 191−200.
(18) Schwieger, W.; Bergk, K.-H.; Heidemann, D.; Lagaly, G.; Beneke, K. *Z. Kristallogr.* **1991**, *197*, 1−12.
(19) Bergk, K.-H.; Grabner, P.; Schwieger, W. *Z. Anorg. Allg. Chem.* **1991**, *600*, 139−144.
(20) Beneke, K.; Lagaly, G. *Am. Mineral.* **1977**, *62*, 763−771.
(21) Beneke, K.; Kruse, H.-H.; Lagaly, G. *Z. Anorg. Allg. Chem.* **1984**, *518*, 65−76.

0020-1669/95/1334-0900$09.00/0

of interlamellar water by alcohols[15,22] and exchange of the alkali metal ions by inorganic cations[23-25] and alkylammonium ions.[20,26-28] Proton exchange transforms the silicates into the corresponding crystalline silicic acids which are able to intercalate guest molecules.[15,29-32a]

The monophyllosilicates are a group of silicates which are expected to reach a certain industrial import. δ-$Na_2Si_2O_5$ is expected to be produced in technical scale and used as a builder in detergents. An other area of interest is the convertion of the silicates into porous materials.[32b]

Methods

Preparation of Silinaite. Dispersions of silica (Kieselgel, Merck Comp., 86.2% SiO_2) in aqueous solutions of LiOH and NaOH were allowed to stand at temperatures between 70 and 125 °C for days or even weeks (Table 2). A well-crystallized silinaite was obtained, for example, from the dispersion of 1 mol of SiO_2 in a solution of 0.6 mol of LiOH and 0.6 mol of NaOH in 20 mol of water at 90 °C for 10 days. We used thick-walled Teflon flasks with nearly gastight screw-on-type caps. The flasks were resistent against the alkali metal hydroxides and allowed syntheses at a modest pressure above atmospheric (at 125 °C). Several dispersions were boiled under reflux at 100 °C. The precipitates were washed with small amounts of water and air-dried. Intensive washing was avoided because it initiated a certain exchange of protons for alkali metal ions.

Crystalline Silicic Acids. The crystalline silicic acids were obtained by dispersing air-dried samples of the silicate in an excess of mineral acids with concentrations ranging from 0.1 M to 7 M. In standard runs 0.1 M hydrochloric acid was used. One day later, the solid was separated, washed with water and air-dried.

Intercalation into the Crystalline Silicic Acid. Samples of the air-dried crystalline silicic acid were dispersed in the liquid guest compound (e.g. alcohols, amines). The mixtures were transferred into small lock-up glass tubes and allowed to stand at least 24 h at room temperature or 65 °C before Debye–Scherrer X-ray powder diagrams were taken. Solid state intercalation[33] was carried out by grinding the crystalline silicic acid together with the solid guest compound (e.g. imidazole) in an agate mortar for about 15 min.

Thermal Behavior. Samples of about 100 mg of silinaite or silicic acid were heated to temperatures between 50 and 1200 °C. The weight loss of the samples was measured in two series of experiments. In one series the same sample was heated stepwise to increasing temperatures. In the other run the samples were heated directly from room temperature to the desired higher temperature. In both cases, the weight loss was determined by holding the sample at the desired temperature for 24 h. The X-ray powder diagrams were taken after cooling down the samples to room temperature (over P_4O_{10} in a desiccator). The DTA-TG diagrams were obtained in a thermoanalyzer (STA 429, Netzsch Co., Germany).

Table 2. Formation of Silinaite

run	molar ratios $LiOH/SiO_2$	$NaOH/SiO_2$	H_2O/SiO_2	conditions	products[a]
91 M	0.17	0.17	6.7	90 °C, 67 d	amorphous
91 T	0.20	0.20	12	90 °C, 59 d	M
91 H	0.20	0.20	24	90 °C, 67 d	M
87 E	0.25	0.25	10	125 °C, 6 d	LSS
89 H	0.30	0.30	10	90 °C, 25 d	LSS
89 L	0.30	0.30	30	90 °C, 150 d	M
87 U	0.33	0.33	13	90 °C, 29 d	LSS
87 T	0.40	0.40	16	90 °C, 13 d	LSS
88 Z	0.45	0.45	18	90 °C, 30 d	LSS
88 G	0.5	0.5	10	90 °C, 7 d	S
89 X	0.5	0.5	10	125 °C, 4 d	S
86 G	0.5	0.5	20	90 °C, 60 d	S
89 D	0.5	0.5	20	100 °C,[b] 51 h	LSS
88 N	0.5	0.5	20	125 °C, 4 d	S
88 H	0.5	0.5	30	90 °C, 14 d	LSS
88 K	0.5	0.5	50	90 °C, 39 d	LSS
88 L	0.5	0.5	100	90 °C, 26 d	LSS
88 Y	0.56	0.56	22	90 °C, 6 d	S
89 A	0.59	0.59	24	90 °C, 30 d	S
88 X	0.63	0.63	25	90 °C, 30 d	S
87 S	0.66	0.66	27	90 °C, 21 h	S
89 U	0.7	0.7	20	125 °C, 96 h	S + LS
89 P	0.8	0.8	30	90 °C, 45 d	S + LS
89 N	0.8	0.8	10	90 °C, 45 d	LS
87 R	1	1	40	90 °C, 21 d	(S)
88 F	2	2	80	90 °C, 39 d	amorphous
90 A	0.1	0.9	20	90 °C, 40 d	S
90 B	0.2	0.8	20	90 °C, 7 d	S
89 S	0.3	0.7	20	90 °C, 20 d	S
90 T	0.6	0.4	20	90 °C, 22 d	LSS
89 R	0.7	0.3	20	90 °C, 20 d	LSS
89 T	0.7	0.3	10	90 °C, 20 d	LSS
90 R	0.8	0.2	20	90 °C, 33 d	LSS + LS
90 P	0.9	0.1	20	90 °C, 33 d	LSS + LS

[a] Key: S, silinaite; LSS, lithium sodium silicate; LS, Li_2SiO_3; M, magadiite. [b] Boiled under reflux.

Further Methods. The X-ray powder diagrams were obtained with a Siemens Kristalloflex 810 and by the Debye-Scherrer technique, in both cases with Cu Kα radiation. FT-IR spectra (KBr pellets) were recorded by a Nicolet DX spectrometer.

The MAS-NMR spectra were taken with the Bruker instrument A 400 (HPDEC, MAS 5 kHz, time between two pulses 60 s; cf ref 34).

Gas adsorption isotherms were measured with an automatic gas adsorption apparatus.[35,36] The specific surface area was derived from the desorption branch. Microporosity was determined by *t*-plots. The standard isotherm required for the *t*-plot was constructed as proposed by Lecloux and Pirard[37] for c_{BET} constants 40–100. The external specific surface area of the microporous samples was obtained from the *t*-plot.

The analytical composition was measured by leaching the samples with 0.1 M HCl and determination of Li^+ and Na^+ by DCP emission spectroscopy (Spectra Span IV, Beckmann). The silicon content in the residue ($=SiO_2{\cdot}xH_2O$) cannot be obtained from the weight loss after heating because water may not be quantitatively desorbed (see below and Figure 7). Therefore, the silicon content was measured (by DCP) after dissolution of the residue in boiling soda solution.

Results

Synthesis of Silinaite. Silinaite is synthesized by heating dispersions of silica in aqueous solutions of LiOH and NaOH

(22) Bergk, K.-H.; Schwieger, W.; Schäfer, A. *Z. Chem.* **1989**, *29*, 151–152.
(23) Wolf, F.; Schwieger, W. *Z. Anorg. Allg. Chem.* **1979**, *457*, 224–228.
(24) Bergk, K.-H.; Nietzold, G.; Schwieger, W. *Z. Chem.* **1988**, *28*, 78.
(25) Bergk, K.-H.; Schütz, C.; Schwieger, W. *Silikattechnik* **1990**, *41*, 241–243.
(26) Lagaly, G.; Beneke, K.; Weiss, A. *Proceedings of the International Clay Conference, Madrid, 1972*; Serratosa, J. M., Ed.; Division de Ciencias CSIC: Madrid, 1973; pp 663–673.
(27) Dörfler, H.-D.; Bergk, K.-H.; Müller, K.; Müller, E. *Tenside Deterg.* **1984**, *21*, 226–234.
(28) Dailey, J. S.; Pinnavaia, T. J. *Chem. Mater.* **1992**, *4*, 855–863.
(29) Lagaly, G. *Adv. Colloid Interf. Sci.* **1979**, *11*, 105–148.
(30) Döring, J.; Beneke, K.; Lagaly, G. *Colloid Polym. Sci.* **1992**, *270*, 609–616.
(31) Döring, J.; Lagaly, G. *Clay Miner.* **1993**, *28*, 39–48.
(32) (a) Döring, J.; Lagaly, G.; Beneke, K.; Dékány, I. *Colloids Surf. A* **1993**, *71*, 219–231. (b) Inagaki, S.; Fukushima, Y.; Kuroda, K. *J. Chem. Soc., Chem. Commun.* **1993**, 680–682. Inagaki, S.; Fukushima, Y.; Okada, A.; Kurauchi, T.; Kuroda, K.; Kato, C. *Proceedings of the 9th International Zeolite Conference, Montreal, 1992*; von Ballmoos, R., et al.; Eds.; Butterworth-Heinemann: 1993; pp 305–311.
(33) Ogawa, M.; Shirai, H.; Kuroda, K.; Kato, C. *Clays Clay Miner.* **1992**, *40*, 485–490.
(34) Scholzen, G.; Beneke, K.; Lagaly, G. *Z. Anorg. Allg. Chem.* **1991**, *597*, 183–196.
(35) Kruse, H.-H.; Lagaly, G. *GIT Fachz. Lab.* **1988**, *32*, 1096–1100.
(36) Kruse, H.-H.; Beneke, K.; Lagaly, G. *Colloid Polym. Sci.* **1989**, *267*, 844–852.
(37) Lecloux, A.; Pirard, J. P. *J. Colloid Interface Sci.* **1979**, *70*, 265–281.

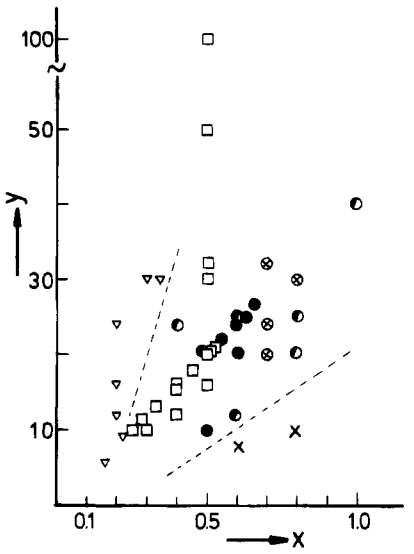

Figure 1. Preparation of silinaite from dispersions of SiO_2 in aqueous NaOH and LiOH solutions at 90−125 °C. y = molar ratio H_2O/SiO_2; x = molar ratio $NaOH/SiO_2 = LiOH/SiO_2$. Key: (●) silinaite; (◐) silinaite, badly crystallized; (□) lithium sodium silicate; (▽) magadiite; (×) Li_2SiO_3; (⊗) silinaite + Li_2SiO_3.

Table 3. Influence of Anions in Silinaite Synthesis

run	mol per mol of SiO_2			conditions	products[a]
86 G	0.5 LiOH	0.5 NaOH	20 H_2O	90 °C, 60 d	S
88 N	0.25 Li_2CO_3	0.5 NaOH	20 H_2O	90 °C, 60 d	M
88 O	0.5 LiOH	0.25 Na_2CO_3	20 H_2O	90 °C, 55 d	M
88 P	0.25 Li_2CO_3	0.25 Na_2CO_3	20 H_2O	90 °C, 143 d[b]	M
88 R	0.5 $LiNO_3$	0.5 NaOH[c]	20 H_2O	90 °C, 143 d[b]	M + LSS
88 S	0.5 LiOH	0.5 $NaNO_3$[c]	20 H_2O	90 °C, 132 d	M
91 W	1.3 LiOH	0.9 NaCl	170 H_2O	90 °C, 41 d	LSS

[a] Key: S, silinaite; LSS, lithium sodium silicate; M, magadiite. [b] Below 143 d: amorphous. [c] pH = 11.

to 90−125 °C for several days (Figure 1). Four crystalline phases were identified by X-ray diffractometry in the system $NaOH-LiOH-SiO_2-H_2O$ at 75−125 °C: sodium lithium silicate with a molar ratio $Li^+/Na \approx 1$; lithium sodium silicate with $Li^+/Na^+ \geq 1.5:0.5$; magadiite; and Li_2SiO_3 (d(Å), (I)): 4.675 (74); 3.296 (100); 2.697 (69); 2.330 (63); 2.083 (10); 1.764 (20)) (Figure 1; Tables 2 and 3).

The sodium lithium silicate is silinaite. Its X-ray powder diagram agrees with the diagram of natural silinaite[8] (Table 4). The lithium sodium silicate is distinguished from silinaite mainly by a poorer resolution of the three reflections around $2\theta = 21.3°$ (Figure 2).[38] X-ray powder patterns intermediate between the extremes shown in Figure 2 are rarely observed. Because of the different coordination (octahedral for Na^+, tetrahedral for Li^+) substitution of sodium by lithium ions cannot occur without structural rearrangements. The tetrahedral silicate layers can cling to the smaller cations by a higher degree of convolution (cf. ref 11, p 199 ff).

The conditions of formation of silinaite from dispersions containing equal molar amounts of NaOH and LiOH at 90 °C−125 °C are evident from Figure 1. Silinaite forms at molar ratios $NaOH/SiO_2 = LiOH/SiO_2$ between 0.5 and 0.7 and water contents between 10 and 28 mol of H_2O/mol of SiO_2. The lithium sodium silicate forms at smaller $NaOH(=LiOH)/SiO_2$ ratios. Below $NaOH(=LiOH)/SiO_2 = 0.25$ magadiite is precipitated (Table 2). LiOH/NaOH ratios below 1 favor formation of silinaite whereas lithium sodium silicate is obtained at LiOH/NaOH ratios above 1 (Table 2). Formation of the silicates needs 4 days at 125 °C and 6−7 days at 90 °C when $NaOH(=LiOH)/SiO_2 > 0.5$ and 4 days for smaller ratios.

The source of silica was amorphous "Kieselgel" (Merck Co., Germany) but other forms (including tetraalkoxysilanes such as tetraethoxysilane) can also be used. For highly dispersed materials (e.g. Aerosil, Degussa) larger amounts of water (>30 mol of H_2O/mol of SiO_2) are required to disperse the silica, and formation of lithium sodium silicate is promoted (cf. Figure 1).

(38) Thiesen, P.; Heidemann, D.; Beneke, K.; Lagaly, G. Manuscript in preparation.

Table 4. X-ray Powder Data of Synthetic and Natural Silinaite[a]

run 89 A		calcd		natural	
I	d (Å)	I	d (Å)	I	d (Å)
		19	7.200		
24	7.162			100	7.14
		38	7.143		
40	4.240	48	4.240	80	4.24
94	4.133	100	4.135	100	4.14
35	4.014	37	4.013	80	4.02
12	3.598	9	3.599	20	3.599
9	3.576	9	3.571	20	3.574
4	3.366	9	3.364	10	3.366
17	3.211	18	3.208	20	3.208
		26	3.046	20	3.046
100	3.014	87	3.011	20	3.014
53	2.850	50	2.849	100	2.847
42	2.700	32	2.703	50	2.698
22	2.515	16	2.513	20	2.514
		8	2.480	20	2.484
12	2.465	9	2.462	20	2.464
13	2.419	11	2.417	20	2.417

[a] Data of natural silinaite and calculated values are from ref 8.

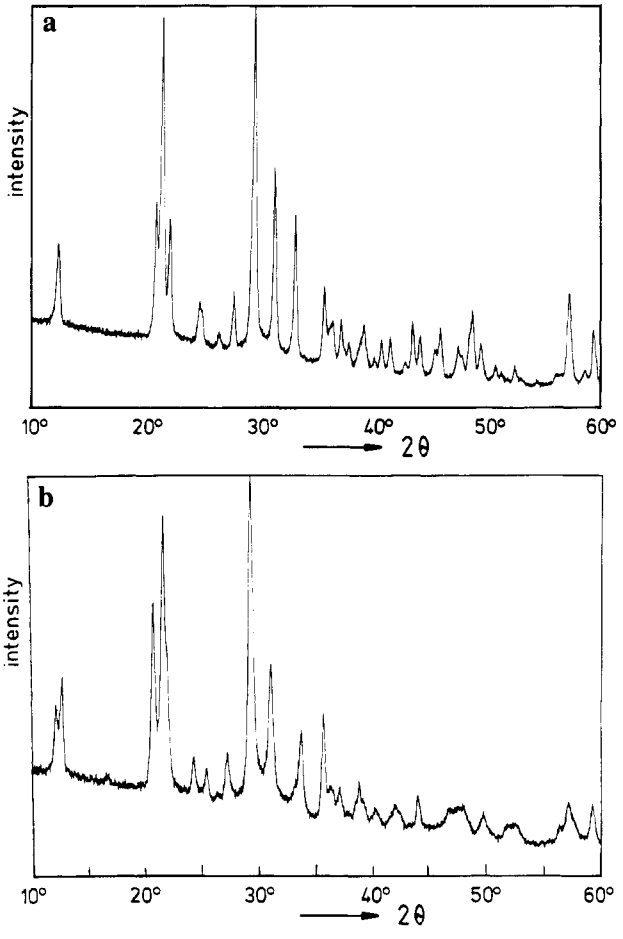

Figure 2. X-ray powder pattern of synthetic silinaite (sample 89 A) (a) and lithium sodium silicate (sample 88 H) (b).

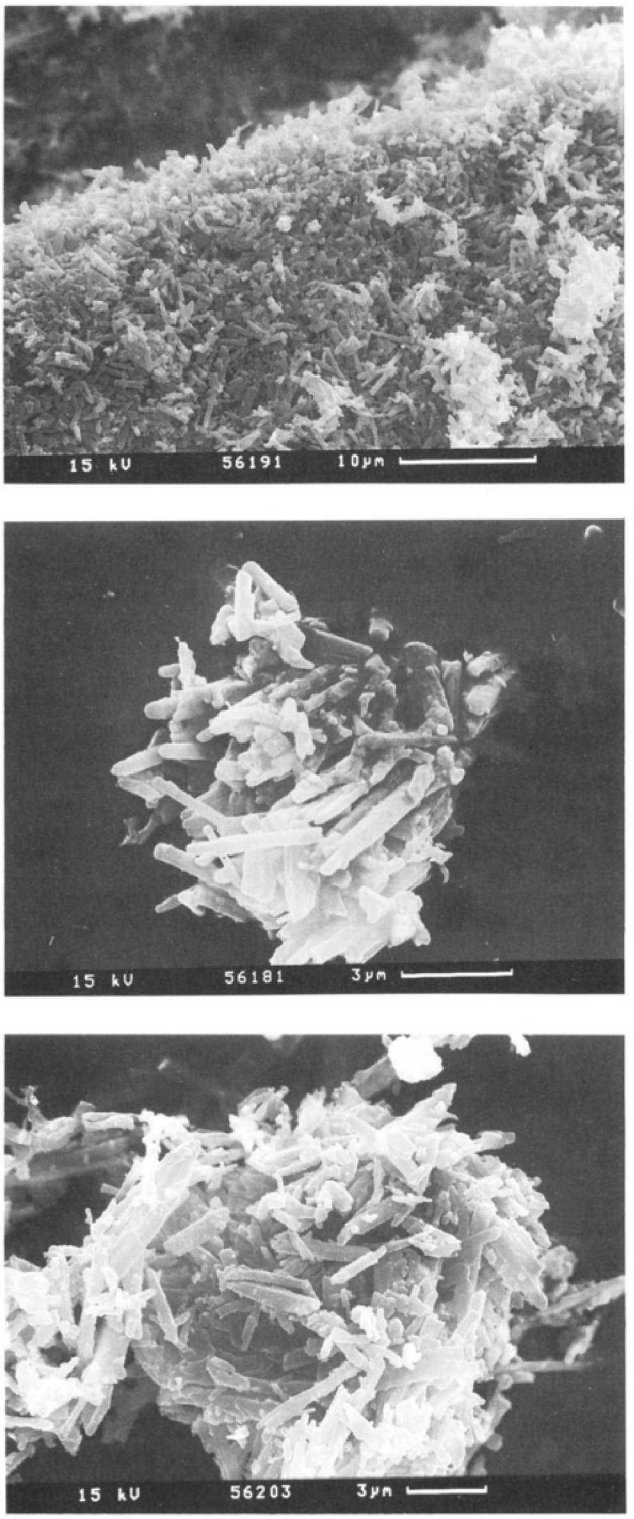

Figure 3. Scanning electron micrographs (top to bottom) of silinaite, (a) sample 89 X and (b) sample 89 A and of the crystalline silicic acid (c) prepared from sample 89 A with 7 M HNO_3.

The type of anion influences the reaction rate and the nature of the sodium silicate. Carbonate ions promote formation of the more highly condensed kenyaite on the expense of magadiite.[39] They also impede formation of silinaite, and magadiite is obtained (Table 3). Replacement of OH^- by NO_3^- leads to amorphous products or magadiite. Substitution of NaOH by KOH yields the potassium lithium form of $K_2H_2Si_{20}O_{42}{\cdot}xH_2O$.[14,21]

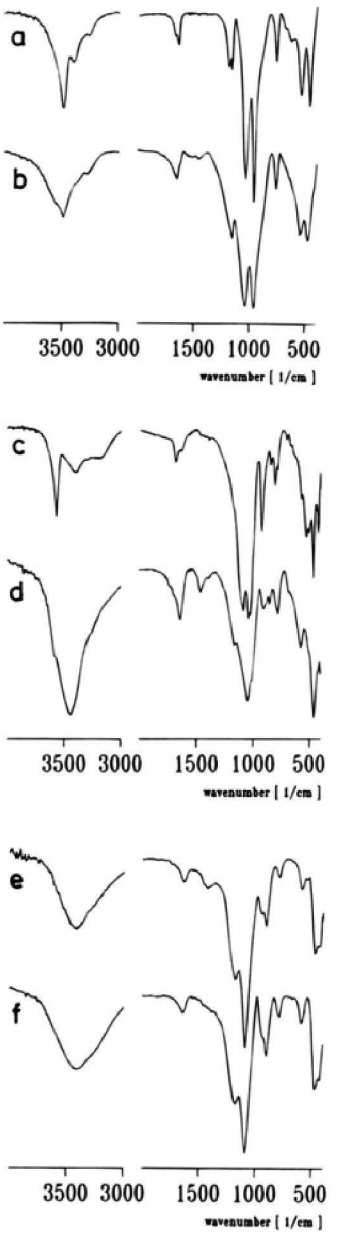

Figure 4. FT-IR spectra of silinaite (sample 89 A) (a), lithium sodium silicate (sample 87 U) (b), makatite (c), kanemite (d) and of the H^+ forms of sample 89 A (e) and sample 87 U (f) (all samples air-dried).

Properties of Synthetic Silinaite. Silinaite and the lithium sodium silicate form lath shaped particles a few micrometers long (Figure 3).

Silinaite is identified in the X-ray diffraction diagram by a group of three reflections around $2\theta = 21.3°$ ($d = 4.25-4.03$ Å) (Figure 2; Table 4). The diagrams of the samples of synthetic silinaite are very similar and show only modest differences in crystallinity. The *d*-values agree with the calculated values and also with the *d*-values of the natural sample.[8] The intensities of the synthetic silinaites agree better with the calculated intensities than those of the natural sample.

The IR spectrum of silinaite in the region of OH stretching vibrations shows a sharp and intense band at 3490 cm^{-1} and two well developed bands at 3399 and 3272 cm^{-1} (Figure 4a), which are assigned as stretching vibrations of the interlamellar water molecules. A group of well-developed bands is typical of water molecules in crystalline hydrates.[40] An increasing

(39) Fletcher, R. A.; Bibby, D. M. *Clays Clay Miner.* **1987**, *35*, 318–320.

(40) Siebert, H. *Anwendungen der Schwingungsspektroskopie in der anorganischen Chemie*; Springer Verlag: Berlin, 1966.

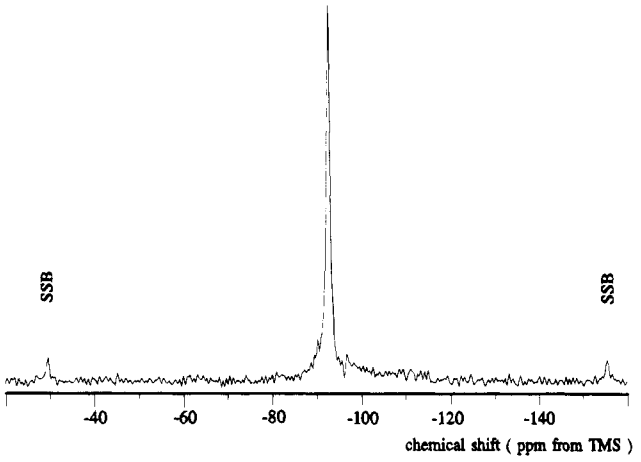

Figure 5. ^{29}Si MAS NMR spectrum of silinaite (sample 89 A, air-dried). SSB = spinning side bands.

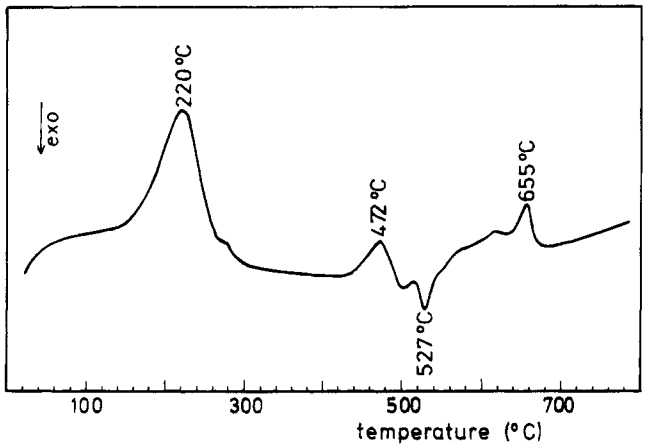

Figure 6. DTA diagram of synthetic silinaite (sample 86 G).

diversification of the hydrogen bonds (silinaite; makatite → kanemite → magadiite; kenyaite) converts the individual bands into a broadened absorption band (Figure 4a–d) (for magadiite and $K_2H_2Si_{20}O_{42}{\cdot}xH_2O$ see refs 34, 41). The IR spectra of the lithium sodium silicates are somewhat poorer resolved (Figure 4b), and the band around 3484 cm^{-1} is broadened in comparison with silinaite.

According to the crystal structure all Si sites in silinaite are crystallographically equivalent. In fact, the ^{29}Si MAS-NMR spectrum shows one signal only with a chemical shift of 92.4 ppm (related to tetramethyl silicate) (Figure 5). The chemical shift is typical for Q^3 groups ($Na_2Si_2O_5$, α-form −94.3 ppm, β-form, −86.7 and 88.6 ppm, δ-form −90.4 ppm;[42] makatite, −93.6 ppm[18]). The two small peaks are spinning side bands.

Thermal Dehydration of Silinaite. A large endothermic peak in the DTA diagram, beginning at 120 °C, indicates the desorption of interlamellar water (Figure 6). The X-ray powder diagram of the samples heated to 120–400 °C is different from that of silinaite. This is understandable because only a few weak (*hk*0) reflections are seen in the powder diagram. Only these reflections would persist when the lattice constant *c* decreases as a consequence of interlamellar water desorption. A second endothermic peak at 470 °C followed by a small exothermic peak and the significantly different X-ray powder diagram indicate further structural changes. The endothermic peak at 655 °C is related to the melting of the silicate.

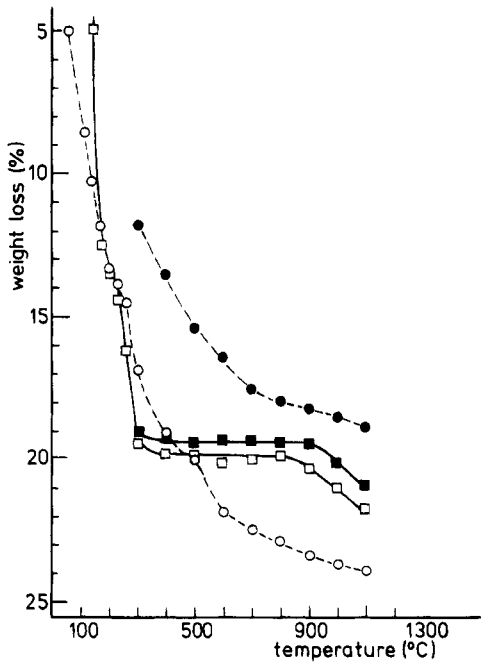

Figure 7. Weight loss curves for silinaite (sample 86 G) and its H^+ form: (□) silinaite, heated stepwise from room temperature to 1100 °C; (■) silinaite, heated to 300 °C, then stepwise to 1100 °C; (○) H^+ form, heated stepwise from room temperature to 1100 °C; (●) H^+ form, heated to 300 °C and then stepwise to 1100 °C.

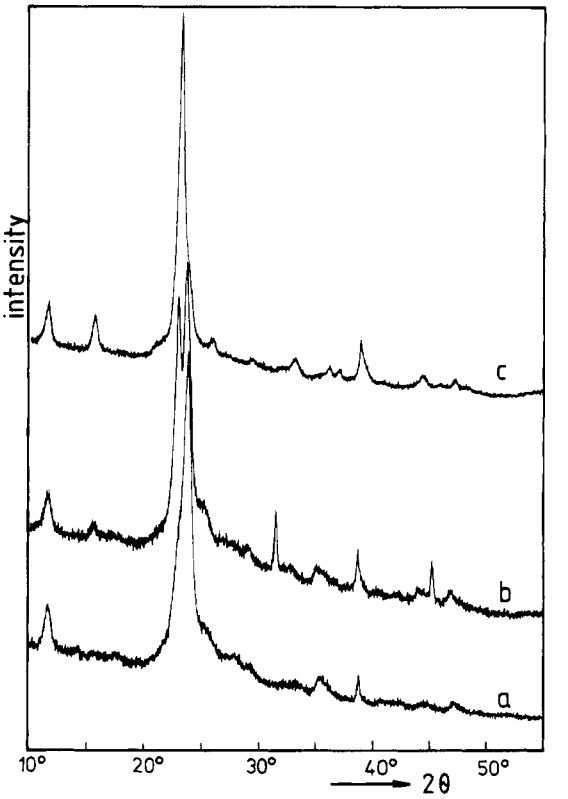

Figure 8. X-ray powder diagrams of crystalline acids obtained from synthetic silinaite and lithium sodium silicate: (a) H^+ form of silinaite (from sample 87 U, 7 M HNO_3); (b) mixture of the H^+ form of silinaite and α-$H_2Si_2O_5$ (from sample 89 A, 0.1 M HCl); (c) α-$H_2Si_2O_5$ (from sample 89 X, 0.1 M HCl).

A sample heated to 140 °C (highest *d*-value 6.35 Å) and then dispersed in water rehydrates to silinaite. Samples heated to 170 and 200 °C and rehydrated show only weak reflections of silinaite among the more intense reflections of the 6.35-Å phase.

(41) Rojo, J. M.; Ruiz-Hitzky, E.; Sanz, J. *Inorg. Chem.* **1988**, *27*, 2785–2790.
(42) Heidemann, D.; Hübert, C.; Schwieger, W.; Grabner, P.; Bergk, K.-H.; Sarv, P. *Z. Anorg. Allg. Chem.* **1992**, *617*, 169–177.

Table 5. X-ray Powder Data

(a) Crystalline Acids from Different Samples of Synthetic Silinaite and α-$Na_2Si_2O_5$

H^+-silinaite (from 87 U)		H-86 G		H-89 A		H-89 X		α-$H_2Si_2O_5$[49]	
I	*d* (Å)	*I*	*d* (Å)	*I*	*d* (Å)	*I*	*d* (Å)	*I*	*d* (Å)
11	7.540	13	7.591	14	7.537	12	7.619	50	7.69
				5	5.657	10	5.654	50	5.67
7	5.054								
		62	3.846	85	3.865	100	3.859	100	3.87[a]
100	3.716	100	3.719	100	3.748				
		17	3.506	12	3.506	4	3.433	20	3.45
5	3.161							20	3.06
				20	2.825	4	2.706	50	2.718
8	2.531	9	2.537	6	2.548	4	2.488	30	2.485
						2	2.423		
18	2.319	20	2.317	15	2.318	11	2.319	40	2.318
4	2.016			15	1.997	3	2.046	40	2.065
4	1.927			5	1.930	3	1.927		

(b) Monophyllosilicic Acids $H_2Si_2O_5$[b]

β-$H_2Si_2O_5$[50] from β-$Na_2Si_2O_5$		β′-$H_2Si_2O_5$[49] from β-$Na_2Si_2O_5$		$H_2Si_2O_5$[46] from $KHSi_2O_5$		$H_2Si_2O_5$[3] from kanemite		$H_2Si_2O_5$[c] from makatite		$H_2Si_2O_5 \cdot 0.7H_2O$[d] from copper silicate	
I	*d* (Å)	*I*	*d* (Å)	*I*	*d* (Å)	*I*	*d* (Å)	*I*	*d* (Å)	*I*	*d* (Å)
5	7.43	s[e]	7.75	60	5.97	90	6.00	13	7.62	100	9.65
100	5.485	w	6.94	15	4.67	30	4.666	7	6.875	30	6.41
2	4.502	ww	5.42	20	4.10	50	4.101	3	5.399	2	5.90
30	4.236	m	5.24	100	3.76	100	3.77	8	4.378	80	4.85
50	4.055	ms	4.67	25	3.39	60	3.388	17	4.256	5	4.72
30	3.842	s	3.99	40	3.17	70	3.170	44	3.837	10	3.88
15	3.682	m	3.70	2	3.00	50	2.858	100	3.744	15	3.64
50	3.552	m	3.56	20	2.864	40	2.770	67	3.352	30	3.42
20	3.145	mw	3.32	17	2.765	50	2.662	9	3.077	70	3.35
25	2.950	mw	3.16	25	2.660	10	2.549	8	2.797	40	3.17
		ss	3.00	2	2.545	70	2.454	6	2.675	40	3.02
30	2.479	w	2.873	40	2.455			6	2.645		
		m	2.725					3	2.531		

[a] Broadened reflection. [b] α-$H_2Si_2O_5$ see part a. [c] From synthetic makatite, run 29 W; see also ref 18. [d] From $Na_2CuSi_4O_{10}$ or $NaKCuSi_4O_{10}$ (litidionite).[51] [e] Intensities: ss (very strong) > s > ms > m > mw > w > ww (very weak).

After heating to 230−400 °C the 6.35-Å phase no longer rehydrates into silinaite.

The desorption of water above 100 °C is accompanied by a considerable weight loss (Figure 7). The weight remains constant between 300 and 900 °C in spite of the structural changes at 470 °C and the melting of the sample at 650 °C. A considerable desorption of the alkali metal oxides, mainly Na_2O, greatly reduces the weight above 1000 °C.

The desorption of water from the interlayer space is often influenced by kinetic effects, and DTA and DTG data are not related to equilibrium states. When the samples are rapidly heated to a higher temperature, the layers collapse at the crystal edges and water remains trapped in the particle core.[21] Reliable weight loss curves are obtained by heating a sample at 110 °C for 24 h, then 24 h at the next desired temperature (140 °C in Figure 7) and so on. A sample heated directly to 300 °C and subsequently to 400 and 500 °C, etc., shows a smaller weight loss due to the trapping of water between the collapsing layers.

The weight loss of 19.9% (Figure 7) corresponds to a water content of 2.29 mol of H_2O/mol of $NaLiSi_2O_5$. The natural sample had the composition $NaLiSi_2O_5 \cdot 2H_2O$.[8,9] The theoretical interlamellar water content is $5.06 \times 8.33/(2 \times 10.5) = 2$. (The unit cell with $a = 5.06$ Å, $b = 8.33$ Å, and $c = 2 \times 7.19$ Å contains 4 formula units. The area of a water molecule in water monolayers in smectites is 10.5 Å^2 (3500 m^2/g of H_2O).)[43]

The H^+ Form of Silinaite. Exchange of the Li^+ and Na^+ ions of silinaite and the lithium sodium silicate with mineral acids often produces a mixture of two crystalline silicic acids (Figure 8, Table 5). One acid is α-$H_2Si_2O_5$, the other is considered the H^+ form of silinaite. The powder diagram of this acid is given in Table 5a. The presence of both forms of $H_2Si_2O_5$ is easily detected in the X-ray powder diagram by the intense reflections at $2\theta = 25-30°$ (H^+ form of silinaite, $d \approx 3.72$ Å; α-$H_2Si_2O_5$ $d \approx 3.87$ Å) (Figures 8 and 9; Table 5a). As silinaite and α-$H_2Si_2O_5$[44] consist of the same type of zweier single layers but with different degree of convolution, transformation into α-$H_2Si_2O_5$ proceeds by stronger folding of the tetrahedral layers. A mixture of different modifications of $H_2Si_2O_5$ was also obtained when kanemite was reacted with mineral acids.[20]

The nature of the product after the Li^+, $Na^+ \rightarrow H^+$ exchange depends on the concentration of the acid. Generally, more highly concentrated acids (e.g. 7 M HNO_3, 6 M HCl) give the H^+ form of silinaite whereas diluted acids promote transformation into α-$H_2Si_2O_5$. For instance, sample 89 X (well crystallized silinaite) gives the H^+ form of silinaite in 6 M HCl and 7 M HNO_3 and α-$H_2Si_2O_5$ in 0.1 M HCl (Figure 9).

When the Na^+ and Li^+ ions are reacted with concentrated acids (HCl, HNO_3, H_2SO_4), the X-ray powder diagram of the samples in contact with the acids is often badly developed. It exhibits sharper and more intense reflections after washing and air-drying. The quality of the powder diagram is again lost after redispersion of the acid in water. This is a strong indication of a certain degree of delamination of the dispersed phyllosilicic acid (disarticulation of the crystals into the individual layers or

(43) Kraehenbuehl, F.; Stoeckli, H. F.; Brunner, F.; Kahr, G.; Mueller-Vonmoos, M. *Clay Miner.* **1987**, *22*, 1−9.

(44) Liebau, F. *Z. Kristallogr.* **1964**, *120*, 427−449.

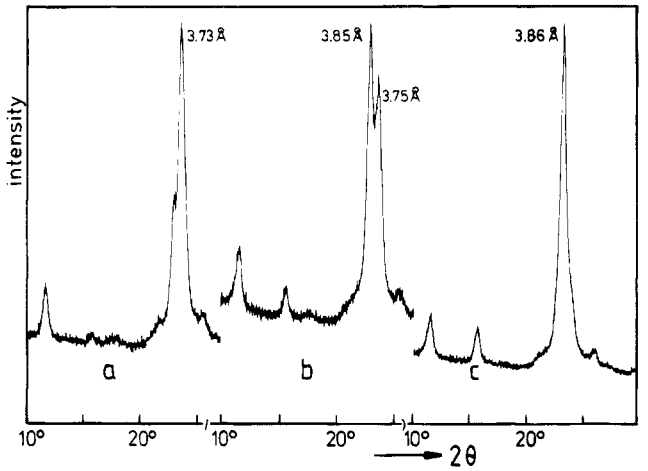

Figure 9. Transformation of silinaite (sample 89 X) into crystalline silicic acids with mineral acids of different concentrations at room temperature: (a) 7 M HNO_3 or 6 M HCl; mainly H^+ form of silinaite; (b) 1.2 M HCl or 0.5 M H_2SO_4; mixture of the H^+ form of silinaite and α-$H_2Si_2O_5$; (c) 0.1 M HCl; α-$H_2Si_2O_5$. (The reflection at $2\theta \approx 23.8°$ ($d \approx 3.73$) is from the H^+ form of silinaite, that at $2\theta \approx 23.0°$ ($d \approx 3.86$) is from α-$H_2Si_2O_5$.)

packets of them)[30,45] as a consequence of the attack by the concentrated acids.

As for other disilicic acids[46,47] the IR spectrum of the H^+ form of silinaite exhibits a broad absorption band between 3000 and 3600 cm^{-1} (Figure 4e,f) due to the hydrogen bonds on and between the layers.

Transformation of the silicate into the acid does not alter the particle morphology as seen in scanning electron microscopy (Figure 3c) but greatly changes the gas adsorption properties. N_2 adsorption on silinaite at 77 K gives a type II isotherm with no hysteresis and a small BET surface area (Figure 10a,c). The isotherm of the acid form of this silinaite (Figure 10b) shows the unusual form of hysteresis extending down to very small pressures. The t-plot indicates the presence of micropores. The micropore volume is 25 cm^3 (*STP*)/g; the external surface area is 60 m^2/g. Similar observations were made with the silicate $K_2H_2Si_{20}O_{42}{\cdot}xH_2O$ and its silicic acid.[36] Nitrogen molecules penetrate between the silicate layers at high relative pressure and are not desorbed when the pressure is reduced, even below $p/p_0 < 0.1$. This behavior was not found for α-$H_2Si_2O_5$ and $H_2Si_2O_5$-III.[48] The gas adsorption isotherm of α-$H_2Si_2O_5$ (from silinaite, sample 89 X, with 0.1 M HCl) shows a very small mesopore hysteresis but no hysteresis extending down to $p/p_0 \rightarrow 0$ (Figure 10d). The BET surface area is 118 m^2/g, that of the parent silinaite is 26 m^2/g. The surface area of a sample of α-$H_2Si_2O_5$ increased from 95 to 225 m^2/g within 4 years.[48] Changes in the X-ray powder diagram were not observed. This behavior also illustrates the reduced stability of this acid.

The thermal dehydration of the H^+ form of silinaite (sample 86 G) reveals an interesting behavior in that water is continuously desorbed up to 1100 °C (Figure 7b). The weight loss of 24% at 1000 °C indicates the composition $H_2Si_2O_5{\cdot}1.1H_2O$. The influence of kinetic effects on the thermal dehydration of the acid is still more pronounced than for silinaite. Considerable amounts of water are trapped between the collapsing layers when the acid is directly heated to higher temperatures (Figure 7b).

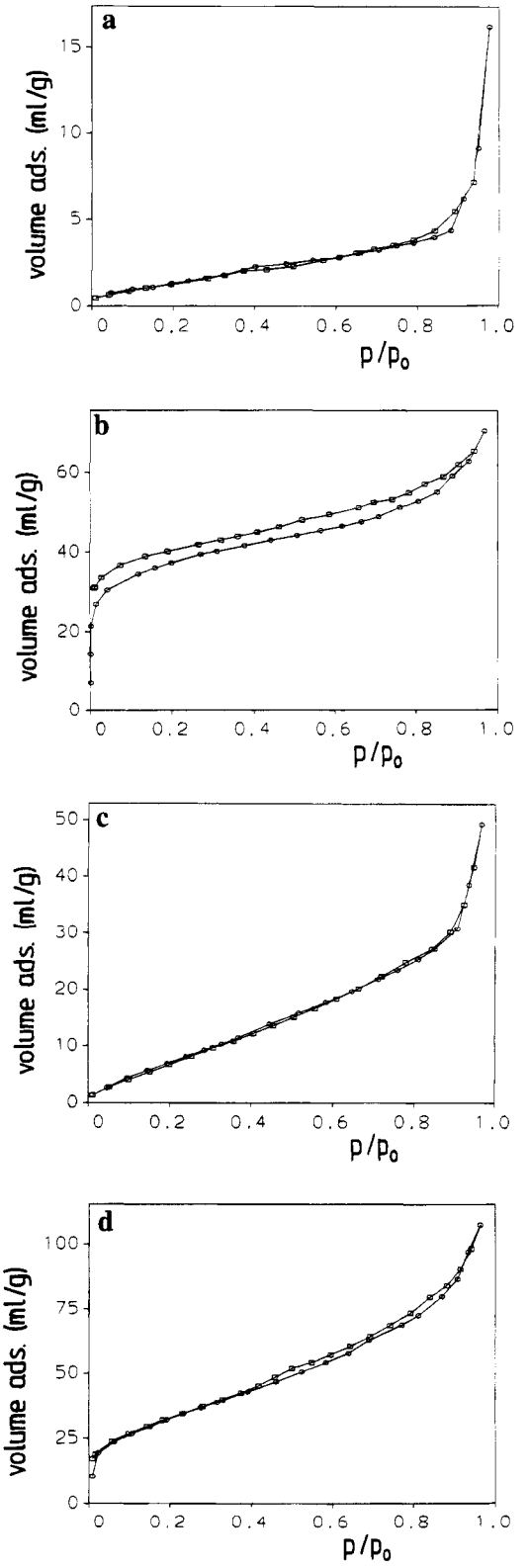

Figure 10. Gas adsorption isotherms (N_2, 77 K): (a) silinaite (sample 86 G), $S = 4.6$ m^2/g, $v_p = 0$; (b) H^+ form of silinaite (from sample 86 G, 0.1 M HCl), $S = 60$ m^2/g, $v_p = 24.8$ cm^3(STP)/g; (c) silinaite (sample 89 X), $S = 26$ m^2/g, $v_p = 0$; (d) α-$H_2Si_2O_5$ from silinaite (sample 89 X, 0.1 M HCl), $S = 117$ m^2/g, $v_p \approx 4$ cm^3(STP)/g. Key: (○) adsorption; (□) desorption; S = specific surface area, v_p = micropore volume).

(45) Lagaly, G.; Beneke, K. *Colloid Polym. Sci.* **1991**, *269*, 1198–1211.
(46) Wey, R.; Kalt, A. *C. R. Acad. Sci. Paris* **1967**, *265*, 1437–1440.
(47) Kalt, A.; Wey, R. *Bull. Groupe Fr. Argiles* **1968**, *20*, 205–214.
(48) Kruse, H.-H. Thesis, University Kiel, 1987.
(49) Hubert, Y.; Guth, J.-L.; Wey, R. *C. R. Acad. Sci. Paris* **1974**, *278*, 1453–1455.
(50) Hubert, Y.; Kalt, A.; Guth, J.-L.; Wey, R. *C. R. Acad. Sci. Paris* **1976**, *282*, 405–408.
(51) Guth, J.-L.; Hubert, Y.; Kalt, A.; Perati, B.; Wey, R. *C. R. Acad. Sci. Paris* **1978**, *286*, 5–8.
(52) Lagaly, G.; Beneke, K.; Dietz, P.; Weiss, A. *Angew. Chem., Int. Ed. Engl.* **1974**, *13*, 819–821.

Table 6. Basal Spacings (d_{001} Values) of the Crystalline Silicic Acid from Silinaite (sample 86G) Where the Basal Spacing of the Dried Acid is 7.59 Å

guest compound	basal spacing (Å)	
	$H_2Si_2O_5$ from silinaite	α-$H_2Si_2O_5$[a]
hexylamine	24.5	24.4
decylamine	34.6	35.0
triethylenediamine	12.7	
hexamethylenediamine	11.2	
ephedrine	18.4	
cyclohexylamine	18.4	18.3
aniline	*b*	22.0
piperazine	10.9	
pyridine *N*-oxide	12.5	12.6
imidazole	12.3	12.6
hydrazine hydrate	10.0	10.0
ammonia	9.7	9.8

[a] From refs 29 and 52. [b] No reaction.

A typical property of crystalline silicic acids is intercalation of certain neutral organic compounds.[29] The reactivity of the H^+ form of silinaite is low but several organic bases are intercalated (Table 6). Pillared derivatives can be prepared as described for the H^+ form of magadiite (reaction of the alkylamine intercalation compound with tetraethoxysilane).[28] Thermal decomposition of the silicic acid–guest compounds provides another way to convert the silicate into highly porous materials.

The reduced intracrystalline reactivity corresponds to the behavior of the silicic acids derived from $Na_2Si_2O_5$, $KHSi_2O_5$, kanemite, and makatite.[20,29] The identity of the basal spacings after intercalation into the H^+ form of silinaite and α-$H_2Si_2O_5$ also illustrates the close relationship between both acids.

Acknowledgment. Thanks are extended to Mrs. M. Mader for taking the X-ray powder diagrams and Dr. Ch. Samtleben, Mr. W. Reimann, and Mrs. U. Schuldt for the scanning electron micrographs. We are grateful to the "Fonds der Chemischen Industrie" for financial support.

IC940652M